SIAM J. SCI. COMPUT.
Vol. 41, No. 6, pp. A3757–A3778

ON ENERGY DISSIPATION THEORY AND NUMERICAL STABILITY FOR TIME-FRACTIONAL PHASE-FIELD EQUATIONS*

TAO TANG†, HAIJUN YU‡, AND TAO ZHOU§

Abstract. For the time-fractional phase-field models, the corresponding energy dissipation law has not been well studied on both the continuous and the discrete levels. In this work, we address this open issue. More precisely, we prove for the first time that the time-fractional phase-field models indeed admit an energy dissipation law of an integral type. In the discrete level, we propose a class of finite difference schemes that can inherit the theoretical energy stability. Our discussion covers the time-fractional Allen–Cahn equation, the time-fractional Cahn–Hilliard equation, and the time-fractional molecular beam epitaxy models. Several numerical experiments are carried out to verify the theoretical predictions. In particular, it is observed numerically that for both the time-fractional Cahn–Hilliard equation and the time-fractional molecular beam epitaxy model, there exists a coarsening stage for which the energy dissipation rate satisfies a power law scaling with an asymptotic power $-\alpha/3$, where α is the fractional parameter.

Key words. time-fractional phase-field equations, Allen–Cahn equation, Cahn–Hilliard equation, MBE model, energy dissipation law, maximum principle

AMS subject classifications. 65M12, 65M06, 35Q99, 74A50

DOI. 10.1137/18M1203560

1. Introduction.

The phase-field method is a powerful modeling and simulation tool in diverse research areas, such as material sciences [5, 9, 10, 26], multiphase flow [6, 31, 32, 33, 39, 42, 51], biology, and tumor growth [13, 20, 27, 49]. Most phase-field formulations are based on a free energy function depending on an order parameter (the phase field) and a diffusive mechanism. The well-known examples of phase-field models include the Allen–Cahn (AC) equation [5], the Cahn–Hilliard (CH) equation [9], and the molecular bean epitaxy (MBE) model [10, 26]. A common feature of the above-mentioned phase-field models is that their corresponding free energy admits a dissipation law.

Taking the CH equation as an example, we see that the associated governing equation yields

$$\begin{cases} \frac{\partial \phi}{\partial t} + \gamma(-\Delta)\left(-\varepsilon\Delta\phi + \frac{1}{\varepsilon}F'(\phi)\right) = 0, \quad x \in \Omega \subset \mathbb{R}^d,\ d = 2, 3, \quad 0 < t \le T, \\ \phi(x, 0) = \phi_0(x), \end{cases} \tag{1.1}$$

*Submitted to the journal's Methods and Algorithms for Scientific Computing section July 27, 2018; accepted for publication (in revised form) August 27, 2019; published electronically November 26, 2019.

https://doi.org/10.1137/18M1203560

Funding: This work was partially supported by the NNSF of China under grants 11688101, 11771439, 91530322, 91630312, 91630203, 11571351, and 11731006; China National Program on Key Basic Research Project 2015CB856003; the Science Challenge Project (TZ2018001); NCMIS; and the Youth Innovation Promotion Association (CAS).

†Division of Science and Technology, BNU-HKBU United International College, Zhuhai, Guangdong, China, and Shenzhen International Center for Mathematics, Southern University of Science and Technology, Shenzhen, 518055 China (tangt@sustech.edu.cn).

‡NCMIS & LSEC, Institute of Computational Mathematics and Scientific/Engineering Computing, Academy of Mathematics and Systems Science, Chinese Academy of Sciences, Beijing, 100190 China, and School of Mathematical Sciences, University of Chinese Academy of Sciences, Beijing, 100190 China (hyu@lsec.cc.ac.cn).

§NCMIS & LSEC, Institute of Computational Mathematics and Scientific/Engineering Computing, Academy of Mathematics and Systems Science, Chinese Academy of Sciences, Beijing, 100190 China (tzhou@lsec.cc.ac.cn).

where ε is an interface width parameter, γ is the mobility, and F is a double-well potential that usually takes the form

$$F(\phi) = \frac{1}{4}(1-\phi^2)^2. \tag{1.2}$$

For simplicity, we set $\Omega = (0, 2\pi)^d$ and assume that $\phi(\cdot, t)$ satisfies a periodic boundary condition. The corresponding free energy functional for the CH equation is defined as

$$E(\phi) := \int_\Omega \Big(\frac{\varepsilon}{2}|\nabla\phi|^2 + \frac{1}{\varepsilon}F(\phi)\Big)dx. \tag{1.3}$$

The CH equation can be viewed as a gradient flow with the energy (1.3) in H^{-1}. It is well known that the energy functional E decreases in time:

$$\frac{d}{dt}E(\phi) = -\int_\Omega \left|\nabla\left(-\varepsilon^2\Delta\phi + F'(\phi)\right)\right|^2 dx \le 0. \tag{1.4}$$

Such an energy dissipation property plays an important role in developing stable numerical methods for dissipation systems due to its importance for long time simulations; see, e.g., [12, 14, 16, 17, 18, 19, 41, 48, 50, 52, 53] and references therein.

In recent years, fractional-type phase-field models have attracted more and more attention [1, 2, 3, 54, 28, 36, 43]. For instance, the following fractional-type free energy is investigated in [43]:

$$E^\alpha(\phi) := \int_\Omega \Big(\frac{\varepsilon^2}{2}|\nabla^\alpha\phi|^2 + F(\phi)\Big)dx, \tag{1.5}$$

where ∇^α is the fractional gradient $\nabla^\alpha = (\frac{\partial^\alpha}{\partial x_1}, \dots, \frac{\partial^\alpha}{\partial x_d})$, with $\{\frac{\partial^\alpha}{\partial x_k}\}_k$ being the fractional derivatives. We are then interested in the following space-fractional CH equation:

$$\frac{\partial\phi}{\partial t} + (-\Delta)\left(-\varepsilon^2\Delta^\alpha\phi + F'(\phi)\right) = 0. \tag{1.6}$$

It is obvious that for the modified energy functional (1.5), the corresponding energy dissipation law is

$$\frac{d}{dt}E^\alpha(\phi) \le 0. \tag{1.7}$$

Another interesting approach is to keep the original free energy (1.3) unchanged, but the associated gradient flow is considered in $H^{-\alpha}$. This yields the following space-fractional CH equation [1]:

$$\frac{\partial\phi}{\partial t} + (-\Delta)^\alpha\left(-\varepsilon^2\Delta\phi + F'(\phi)\right) = 0. \tag{1.8}$$

It is straightforward to verify that its corresponding free energy admits a dissipation law. As reported in [1], the nature of the solution for the fractional CH is qualitatively close to the behavior of the classical CH equation (1.1) regardless of the size of the parameter α.

The time-fractional phase-field models have also been investigated recently. Consider the time-fractional CH equation

$$\frac{\partial^\alpha}{\partial t^\alpha}\phi + \gamma(-\Delta)\Big(-\varepsilon\Delta\phi + \frac{1}{\varepsilon}F'(u)\Big) = 0, \tag{1.9}$$

where $\alpha \in (0,1)$, and $\frac{\partial^\alpha}{\partial t^\alpha}$ is the Caputo derivative defined as

$$\frac{\partial^\alpha}{\partial t^\alpha}\phi = {}_0^C D_t^\alpha \phi(t) := \frac{1}{\Gamma(1-\alpha)}\int_0^t \frac{\phi'(s)}{(t-s)^\alpha}ds, \quad t>0, \quad \alpha\in(0,1). \tag{1.10}$$

In [28], it is shown numerically that the free energy admits an energy dissipation law. However, rigorous analysis for this observed behavior is still open, which is the main motivation of the present work. Our main contribution is threefold:

- In the continuous level, we establish the energy dissipation law for the time-fractional AC equation, the time-fractional CH equation, and the time-fractional MBE model.
- In the discrete level, we propose a class of finite difference schemes satisfying the discrete energy dissipation law for the time-fractional problems.
- We also investigate the coarsening rate of the time-fractional phase-field models, and we obtain an asymptotic value for a power law.

The rest of the paper is organized as follows. In section 2, we establish the energy dissipation law for the time-fractional phase-field equations. In section 3, a class of finite difference schemes is proposed, whose numerical solutions are shown to satisfy the energy dissipation property. In section 4, we discuss the maximum principle for the time-fractional AC equation. Numerical examples will be presented in section 5 to verify our theoretical results and to predict an asymptotic power law. Finally, we give some concluding remarks in section 6.

2. Energy dissipation for time-fractional phase-field equations. First, we introduce some notation and basic properties for fractional calculus; see, e.g., [24, 38]. The Riemann–Liouville fractional integrals for $\alpha\in(0,1)$ on finite interval $[0,T]$ are defined as

$$(I_{0+}^\alpha f)(t) := \frac{1}{\Gamma(\alpha)}\int_0^t \frac{f(s)}{(t-s)^{1-\alpha}}ds \quad \text{for } t\ge 0,$$
$$(I_{T-}^\alpha f)(t) := \frac{1}{\Gamma(\alpha)}\int_t^T \frac{f(s)}{(s-t)^{1-\alpha}}ds \quad \text{for } t\le T.$$

The Liouville fractional integrals on the real axis $\mathbb{R}$ are defined as

$$(I_+^\alpha f)(t) := \frac{1}{\Gamma(\alpha)}\int_{-\infty}^t \frac{f(s)ds}{(t-s)^{1-\alpha}}, \quad \left(I_-^\alpha f\right)(t) := \frac{1}{\Gamma(\alpha)}\int_t^\infty \frac{f(s)ds}{(s-t)^{1-\alpha}}.$$

For $f\in L^p(0,T), g\in L^q(0,T)$, $p\ge 1, q\ge 1$, and $\frac{1}{p}+\frac{1}{q}\le 1+\alpha$ ($p\ne 1$ and $q\ne 1$ when $\frac{1}{p}+\frac{1}{q}=1+\alpha$), the following integration formulas holds [24, Lemma 2.7, p. 76]:

$$\int_0^T (I_{0+}^\alpha f)(t)g(t)dt = \int_0^T f(t)(I_{T-}^\alpha g)(t)dt. \tag{2.1}$$

Moreover, for $f\in L^p(\mathbb{R}), g\in L^q(\mathbb{R})$, $p,q>1$, and $\frac{1}{p}+\frac{1}{q}=1+\alpha$, we have [24, eq. (2.3.22), p. 89]

$$\int_{-\infty}^\infty (I_+^\alpha f)(t)g(t)dt = \int_{-\infty}^\infty f(t)(I_-^\alpha g)(t)dt. \tag{2.2}$$

Furthermore, for $\alpha, \beta > 0$, $\alpha + \beta < 1/p$, and $f \in L^p(\mathbb{R})$, the following semigroup properties for fractional integrals hold [24, Lemma 2.19, p. 89]:

$$(I_+^\alpha I_+^\beta f)(t) = (I_+^{\alpha+\beta} f)(t), \quad (I_-^\alpha I_-^\beta f)(t) = (I_-^{\alpha+\beta} f)(t). \tag{2.3}$$

The Fourier transform for the Liouville factional integrals is given by [24, Property 2.15, p. 90]

$$(\mathcal{F} I_+^\alpha f)(\xi) = \frac{(\mathcal{F} f)(\xi)}{(-i\xi)^\alpha}, \quad (\mathcal{F} I_-^\alpha f)(\xi) = \frac{(\mathcal{F} f)(\xi)}{(i\xi)^\alpha}, \quad \alpha \in (0,1),\ f \in L^1(\mathbb{R}), \tag{2.4}$$

where

$$(\mp i\xi)^\alpha = |\xi|^\alpha e^{\mp i\alpha\pi \mathrm{sgn}(\xi)/2}.$$

For $0 < \alpha < 1$ and $1 < p < 1/\alpha$, the operators I_{0+}^α and I_{T-}^α satisfy the following estimates, which are known as the Hardy–Littlewood theorem [24, Lemma 2.1.b, p. 72]:

$$\|I_{0+}^\alpha f\|_{L^q(0,T)} \le K \|f\|_{L^p(0,T)}, \qquad \|I_{T-}^\alpha f\|_{L^q(0,T)} \le K \|f\|_{L^p(0,T)}, \tag{2.5}$$

where $q = p/(1-\alpha p)$, and K is a constant independent of f.

Next, we present the following lemma that plays an important role in our analysis.

LEMMA 2.1. *For any given $h \in L^p(0,T)$, $p \ge \frac{2}{1+\alpha}$ with $\alpha \in (0,1)$, define*

$$I_\alpha(h,g) := \frac{1}{\Gamma(\alpha)} \int_0^T \int_0^t \frac{h(s)g(t)}{(t-s)^{1-\alpha}} ds dt.$$

Then the following estimates hold:

$$I_\alpha(h,h) = \int_0^T I_{0+}^\alpha h(t) h(t) dt \ge \cos\frac{\alpha\pi}{2} \|I_{0+}^{\alpha/2} h\|_{L^2(0,T)}^2 \ge 0. \tag{2.6}$$

We briefly outline the proof of the above lemma. It is known that the kernel $1/t^\alpha$ with $\alpha \in (0,1)$ is positive (see, e.g., [34, 35, 37]), and this can be verified by using either the Laplace transform or the Fourier transform. For example, Nohel and Shea [37] present a proof by checking the kernel function's Laplace transform, while the property $I_\alpha(h,h) \ge 0$ is established provided that $h \in C(0,T)$. Here we can extend this result to the space of $h \in L^p(0,T)$ with $p \ge \frac{2}{1+\alpha}$. In this case, (2.6) can be shown by using the Fourier transform technique. To show this, we can perform the zero extension for h from $[0,T]$ to $(-\infty,\infty)$, apply the semigroup property (2.3), and use the integration formula (2.2) to rewrite the integrand of the outer integration as $(I_+^{\alpha/2} h)(I_-^{\alpha/2} h)$. Hence, the desired result (2.6) follows by combining the Fourier transform (2.4), the convolution theorem, and Parseval's theorem with the Hardy–Littlewood inequality (2.5).

Notice that h in Lemma 2.1 is assumed to take values in $\mathbb{R}$. Nevertheless, when h takes values in some Hilbert space, the result can be extended by using the orthonormal bases expansion argument; see, e.g., [35].

A direct extension of Lemma 2.1 leads to the following corollary.

COROLLARY 2.1. *For any given $h, g \in L^p(0,T)$ with $p \ge \frac{2}{2-\alpha}$, define*

$$A_\alpha(h,g) := I_{1-\alpha}(h,g) = \frac{1}{\Gamma(1-\alpha)} \int_0^T \int_0^t \frac{h(s)g(t)}{(t-s)^\alpha} ds dt. \tag{2.7}$$

Then the following estimates hold:

$$A_\alpha(h,h) = \frac{1}{2}\frac{1}{\Gamma(1-\alpha)}\int_0^T\int_0^T \frac{h(s)h(t)}{|t-s|^\alpha}dsdt$$
$$\geq \sin\frac{\alpha\pi}{2}\|I_{0+}^{(1-\alpha)/2}h\|^2_{L^2(0,T)} \geq 0. \tag{2.8}$$

2.1. The time-fractional Allen–Cahn equation. Consider the following time-fractional AC equation:

$$\frac{\partial^\alpha}{\partial t^\alpha}\phi = \gamma\left(\varepsilon\Delta\phi - \frac{1}{\varepsilon}F'(\phi)\right), \quad \alpha\in(0,1), \quad (x,t)\in\Omega\times[0,T], \tag{2.9}$$

with the homogeneous boundary condition

$$\phi(x,t) = 0, \quad (x,t)\in\partial\Omega\times[0,T], \tag{2.10}$$

where ε is the thickness of the phase interface, and γ is a mobility constant. Here we assume that F admits the following property: $F\in C^2(R)$, and there exist two constants $M_1 < 0 < M_2$ such that

$$F'(M_1) = F'(M_2) = 0; \quad F'(u) > 0\ \forall\, u > M_2 \quad \text{and} \quad F'(u) < 0\ \forall\, u < M_1. \tag{2.11}$$

Remark 2.1. The quartic growth double-well potential (1.2) satisfies this property with $M_1 = -1$ and $M_2 = 1$.

Notice that the fractional order $\alpha\in(0,1)$ in (2.9), and when $\alpha = 1$, (2.9)–(2.10) is the standard AC equation, which satisfies a well-known energy dissipation property,

$$\frac{d}{dt}E[\phi] = -\frac{1}{\gamma}\left\|\frac{\partial}{\partial t}\phi\right\|^2, \tag{2.12}$$

or

$$E[\phi(T)] - E[\phi(0)] = -\frac{1}{\gamma}\int_0^T\left\|\frac{\partial}{\partial t}\phi\right\|^2 dt, \tag{2.13}$$

where $E[\phi]$ is the system energy,

$$E\,[\phi] = \frac{\varepsilon}{2}\|\nabla\phi\|^2 + \frac{1}{\varepsilon}\big\langle F(\phi),1\big\rangle. \tag{2.14}$$

Here we use $\langle\cdot,\cdot\rangle$ to denote the $L^2(\Omega)$ inner product in the spatial domain, and we denote by $\|\cdot\|$ the standard $L^2(\Omega)$ norm.

First, we address the question of whether the time-fractional AC equation still satisfies an energy dissipation law similar to (2.12) or (2.13).

THEOREM 2.1. *Consider* (2.9) *with the homogeneous boundary condition* (2.10) *(or homogeneous Neumann/periodic boundary condition); if the initial energy* $E[\phi(0)]$ *is finite, then the following energy holds:*

$$E\,[\phi(T)] - E\,[\phi(0)] = -\frac{1}{\gamma}\int_\Omega A_\alpha(\phi_t,\phi_t)dx \leq 0. \tag{2.15}$$

Proof. Multiplying both sides of (2.9) by $-\phi_t$ and taking integration on the resulting equation yield

$$-\int_0^T \int_\Omega \frac{\partial^\alpha \phi}{\partial t^\alpha}\phi_t dxdt = \gamma \int_0^T \int_\Omega \left(-\varepsilon\Delta\phi + \frac{1}{\varepsilon}F'(\phi)\right)\phi_t dxdt = \gamma \int_0^T \frac{d}{dt}E[\phi]dt.$$

Consequently,

$$E\left[\phi(T)\right] - E\left[\phi(0)\right] = -\frac{1}{\gamma\Gamma(1-\alpha)}\int_\Omega \int_0^T \int_0^t \frac{\phi_t(x,s)}{(t-s)^\alpha} ds\phi_t(x,t)dtdx. \tag{2.16}$$

Then combining (2.16) and Corollary 2.1 yields the desired property (2.15). ∎

Remark 2.2. Notice that (2.15) is an energy dissipation law of integral type, by which we have

$$E[\phi(T)] \le E[\phi(0)].$$

Moreover, the dissipated energy $\frac{1}{\gamma}\int_\Omega A_\alpha(\phi_t,\phi_t)dx$ is also bounded by $E[\phi(0)]$, and thus the solution is energy stable and $\|I_{0+}^{(1-\alpha)/2}\phi_t\|^2_{L^2(0,T)}$ is bounded. However, the conclusion (2.15), in general, does not lead to $\frac{d}{dt}E \le 0$ or $\frac{d^\alpha}{dt^\alpha}E \le 0$.

2.2. The time-fractional Cahn–Hilliard equation. The analysis of the time-fractional AC equation can be extended to the time-fractional CH equation.

THEOREM 2.2. *Consider the potential function F described by* (2.11) *and total energy E defined by* (2.14)*. The time-fractional CH equation*

$$\frac{\partial^\alpha}{\partial t^\alpha}\phi = \gamma\Delta\mu, \quad \mu = -\varepsilon\Delta\phi + \frac{1}{\varepsilon}F'(\phi), \tag{2.17}$$

with periodic boundary conditions or no-flux boundary conditions

$$\frac{\partial\mu}{\partial n}\Big|_{\partial\Omega} = 0, \quad \frac{\partial\phi}{\partial n}\Big|_{\partial\Omega} = 0, \tag{2.18}$$

satisfies the energy dissipation law

$$E\left[\phi(T)\right] - E\left[\phi(0)\right] = -\frac{1}{\gamma}\int_\Omega A_\alpha(\nabla\psi,\nabla\psi)dx \le 0, \tag{2.19}$$

where $\psi = -\Delta^{-1}\phi_t$ is the solution of the equation

$$-\Delta\psi = \phi_t, \tag{2.20}$$

with periodic or homogeneous Neumann boundary condition $\partial_n\psi\big|_{\partial\Omega} = 0$.

Proof. First, we show that the time-fractional CH equation conserves the total mass. More precisely, if ϕ is the solution of (2.17), with the periodic boundary condition or the no-flux boundary condition (2.18), then

$$\int_\Omega \phi(x,t)dx = \int_\Omega \phi(x,0)dx \quad \forall\, t \ge 0. \tag{2.21}$$

To see this, integrate both sides of the first equation in (2.17) in the physical domain to obtain

$$0 = \int_\Omega \frac{\partial^\alpha \phi}{\partial t^\alpha} dx = \frac{1}{\Gamma(1-\alpha)} \int_\Omega \int_0^t \frac{1}{(t-s)^\alpha} \frac{\partial \phi(x,s)}{\partial t} ds dx$$
$$= \frac{1}{\Gamma(1-\alpha)} \int_0^t \frac{1}{(t-s)^\alpha} \left(\int_\Omega \frac{\partial}{\partial t} \phi(x,s) dx \right) ds \quad \forall\, t \geq 0.$$

Then we obtain

$$\frac{d}{dt} \int_\Omega \phi(x,t) dx = \int_\Omega \frac{\partial}{\partial t} \phi(x,t) = 0 \quad \text{for a.e. } t \geq 0.$$

Then (2.21) follows by integrating the above equation. It follows from (2.21) that $\int_\Omega \phi_t dx = 0$. Thus, ψ in (2.20) is well defined. Pairing the first equation of (2.17) with $-\frac{1}{\gamma}\psi$, the second equation with ϕ_t, and summing up the two resulting equations, we get

$$-\frac{1}{\gamma} \left\langle I_{0+}^{1-\alpha} \nabla \psi, \nabla \psi \right\rangle = \frac{d}{dt} E. \tag{2.22}$$

Consequently, the energy dissipation law (2.19) follows by integrating (2.22) from 0 to T and by using Lemma 2.1. ∎

2.3. The time-fractional MBE model. Now we consider the time-fractional MBE model,

$$\frac{\partial^\alpha}{\partial t^\alpha} \phi = \gamma \left(-\varepsilon \Delta^2 \phi + \frac{1}{\varepsilon} \nabla \cdot \mathbf{f}_m(\nabla \phi) \right), \quad \alpha \in (0,1), \tag{2.23}$$

where $\mathbf{f}_m(\mathbf{v}) = \partial F_m(\mathbf{v}) / \partial \mathbf{v}$, and $F_m(\mathbf{v})$ is defined as (see, e.g., [26])

$$F_m(\mathbf{v}) = \begin{cases} \frac{1}{4}\left(|\mathbf{v}|^2 - 1\right)^2 & \text{for model with slope selection,} \\ -\frac{1}{2} \ln \left|1 + |\mathbf{v}|^2\right| & \text{for model without slope selection.} \end{cases} \tag{2.24}$$

It can be verified that $\mathbf{f}_m(\nabla\phi) = (|\nabla\phi|^2 - 1)\nabla\phi$ in the model with slope selection, and $\mathbf{f}_m(\nabla\phi) = -\frac{\nabla\phi}{1+|\nabla\phi|^2}$ in the model without slope selection.

Using arguments similar to those in the last subsection, we can show that the time-fractional MBE model has the following energy dissipation property.

THEOREM 2.3. *If the time-fractional MBE model satisfies periodic boundary condition or no-flux boundary condition*

$$\partial_n \Delta \phi|_{\partial\Omega} = \partial_n \phi|_{\partial\Omega} = 0, \tag{2.25}$$

then the solution of (2.23) *satisfies the energy dissipation law*

$$E_m[\phi(T)] - E_m[\phi(0)] \leq -\frac{1}{\gamma} \int_\Omega A_\alpha(\phi, \phi) dx \leq 0, \tag{2.26}$$

where

$$E_m(\phi) = \frac{\varepsilon}{2} \|\Delta \phi\|^2 + \frac{1}{\varepsilon} \langle F_m(\nabla \phi), 1 \rangle. \tag{2.27}$$

3. Energy stable finite difference schemes. In this section, we design energy stable finite difference schemes for the time-fractional phase-field models. To this end, we first review a commonly used finite difference scheme.

Let us first consider the time-fractional diffusion equation

$$\frac{\partial^\alpha u}{\partial t^\alpha} = \Delta u + g(x,t), \quad \alpha \in (0,1),$$

which can be viewed as a linearized version of the time-fractional AC equation (2.9). For ease of notation, we consider the one-dimensional case, i.e., $\Delta u = \frac{\partial^2 u}{\partial x^2}$, with x being the spatial variable. Let τ be the time step size, and let $t_k = k\tau$, $u^k(\cdot)$ be the numerical approximation of $u(\cdot, t_k)$. By applying the classical L1 scheme (see, e.g., [29, 30]) to the time-fractional derivative and treating other terms in an implicit way, we get the scheme

$$\sum_{j=0}^{k} b_j \frac{u^{k+1-j}(x) - u^{k-j}(x)}{\tau} = \frac{\partial^2 u^{k+1}(x)}{\partial x^2} + g(x, t_{k+1}), \tag{3.1}$$

where

$$b_j = \frac{1}{\Gamma(1-\alpha)} \int_{j\pi}^{(j+1)\pi} \frac{1}{t^\alpha} dt = \frac{\tau^{1-\alpha}}{\Gamma(2-\alpha)} \left[(j+1)^{1-\alpha} - j^{1-\alpha} \right], \quad j \geq 0. \tag{3.2}$$

The derivation of the left-hand side of (3.1) is given as

$$\begin{aligned}
\frac{\partial^\alpha u}{\partial t^\alpha}(x, t_{k+1}) &= \frac{1}{\Gamma(1-\alpha)} \int_0^{t_{k+1}} \frac{u_t(x,s)}{(t_{k+1}-s)^\alpha} ds \\
&= \sum_{j=0}^{k} \frac{u(x,t_{j+1}) - u(x,t_j)}{\tau} \frac{1}{\Gamma(1-\alpha)} \int_{t_j}^{t_{j+1}} \frac{ds}{(t_{k+1}-s)^\alpha} + r_\tau^{k+1} \\
&= \sum_{j=0}^{k} \frac{u(x,t_{j+1}) - u(x,t_j)}{\tau} \frac{\tau^{1-\alpha}}{\Gamma(2-\alpha)} [(k+1-j)^{1-\alpha} - (k-j)^{1-\alpha}] + r_\tau^{k+1} \\
&= \sum_{j=0}^{k} b_{k-j} \frac{u(x,t_{j+1}) - u(x,t_j)}{\tau} + r_\tau^{k+1},
\end{aligned}$$

where the integer derivative $\frac{\partial}{\partial t} u(x,t)$ in time interval $[t_j, t_{j+1}]$ is approximated with a first order Euler scheme [45]. The finite difference scheme for the fractional differential operator is obtained by dropping the remainder r_τ^{k+1}.

Suppose the spatial discretization using the Galerkin approach is accurate enough. Then the H^1 stability is available since the L1 discretization of the fractional derivative satisfies the special property

$$\sum_{j=0}^{k} b_j \frac{u^{k+1-j}(x) - u^{k-j}(x)}{\tau} = \frac{1}{\tau} \left[b_0 u^{k+1} - \sum_{j=0}^{k-1} (b_j - b_{j+1}) u^{k-j} - b_k u^0 \right], \tag{3.3}$$

where

$$b_k > 0, \quad b_k - b_{k+1} > 0, \quad \sum_{j=0}^{k-1} (b_j - b_{j+1}) + b_k = b_0 \quad \forall\ k \geq 0. \tag{3.4}$$

By this property, if we pair the scheme (3.1) with u^{k+1}, then all the cross terms $u^j u^{k+1}$ $(j = 0, \dots, k)$ can be bounded by $\frac{1}{2}[(u^j)^2 + (u^{k+1})^2]$. Hence the H^1 stability can be proved by a simple mathematical induction [30].

Before providing rigorous nonlinear stability analysis, let us make an assumption on the bulk potential function $F(\phi)$: $F(\phi) \in C^2(\mathbb{R})$, and there exists a finite constant L such that

$$\max_{u\in R} |F''(u)| \le L. \tag{3.5}$$

Remark 3.1. There are many ways to modify the potential $F(\phi)$ such that (3.5) is satisfied. One possible way is to lower the far-ends nonlinearity [8, 41, 11, 47]; e.g., we consider the following double-well potential with quadratic growth:

$$F(\phi) = \begin{cases} \frac{11}{2}(\phi-2)^2 + 6(\phi-2) + \frac{9}{4}, & \phi > 2, \\ \frac{1}{4}(\phi^2-1)^2, & \phi \in [-2, 2], \\ \frac{11}{2}(\phi+2)^2 - 6(\phi+2) + \frac{9}{4}, & \phi < -2. \end{cases} \tag{3.6}$$

It can be verified that the above potential satisfies (3.5).

3.1. The time-fractional Allen–Cahn equation. We now consider the time-fractional AC equation (2.9). We adopt the L1 scheme for the linear part of (2.9) and use a stabilization technique for the nonlinear bulk force. This leads to the following semidiscretized scheme for (2.9):

$$\begin{aligned} &\frac{1}{\gamma}\sum_{j=0}^{k} b_j \frac{\phi^{k+1-j}(x) - \phi^{k-j}(x)}{\tau} \\ &\qquad = \varepsilon\Delta\phi^{k+1} - \frac{1}{\varepsilon} f(\phi^k) - \frac{S}{\gamma}(\phi^{k+1} - \phi^k), \quad k \ge 0, \end{aligned} \tag{3.7}$$

where $f(\phi) = F'(u)$, S is a sufficiently large positive constant, $\tau = T/n$ is the time step size, and $\{b_j\}$ are defined by (3.2).

To show the energy stability of the above numerical scheme, we first present the following lemma.

LEMMA 3.1. *For any* $(u_1, \dots, u_n)^T \in \mathbb{R}^n$, *define*

$$B := 2\sum_{k=1}^{n}\sum_{j=1}^{k} b_{|k-j|} u_j u_k.$$

Then we have

$$B = \sum_{k=1}^{n} b_0 u_k^2 + \sum_{k=1}^{n}\sum_{j=1}^{n} b_{|k-j|} u_j u_k \ge \sum_{k=1}^{n} b_0 u_k^2, \tag{3.8}$$

$$B \ge \frac{2}{\tau}\sin\frac{\alpha\pi}{2}\|I_{0+}^{(1-\alpha)/2} u^n(t)\|^2_{L^2(0,T)} + s_n\sum_{k=1}^{n} u_k^2, \tag{3.9}$$

where $s_n = \left(\frac{n+1}{2}\right)^{-\alpha}\frac{1}{\Gamma(1-\alpha)}\tau^{1-\alpha} > 0$, *and the piecewise constant function* $u^n(t)$ *is defined by*

$$u^n(t) = \begin{cases} u_{\lfloor t/\tau\rfloor+1}, & 0 \le t < T, \\ 0 & \textit{otherwise}. \end{cases} \tag{3.10}$$

In (3.10), $\lfloor t\rfloor$ *stands for the integer part of real number* t.

Proof. Note that (3.8) is well known (see, e.g., [25, 46]). We need only prove the inequality (3.9). We prove it by converting B into the form of Corollary 2.1. First, convert $\{u_j, j = 1, \ldots, n\}$ into a piecewise constant function $u^n(t)$ on $[0, T]$ as in (3.10). Obviously, $u^n(t) \in L^2(0, T)$. Then by Lemma 2.1 or Corollary 2.1, we have

$$\begin{aligned}
0 \le \frac{2}{\tau} A_\alpha(u^n, u^n) &= \frac{1}{\tau}\frac{1}{\Gamma(1-\alpha)} \int_0^T \int_0^T \frac{u^n(s)u^n(t)}{|t-s|^\alpha} dsdt \\
&= \frac{1}{\tau}\frac{1}{\Gamma(1-\alpha)} \sum_{k=1}^{n} \int_{(k-1)\tau}^{k\tau} u_k \int_0^T \frac{u^n(s)}{|t-s|^\alpha} dsdt \\
&= \frac{1}{\tau}\frac{1}{\Gamma(1-\alpha)} \sum_{k=1}^{n} u_k \sum_{j=1}^{n} u_j \int_{(k-1)\tau}^{k\tau} \int_{(j-1)\tau}^{j\tau} \frac{1}{|t-s|^\alpha} dsdt = \sum_{k=1}^{n}\sum_{j=1}^{n} u_j u_k \tilde{b}_{|k-j|},
\end{aligned}$$

where

$$\begin{aligned}
\tilde{b}_{|k|} &= \frac{1}{\Gamma(1-\alpha)}\frac{1}{\tau} \int_{k\tau}^{(k+1)\tau} \int_0^\tau \frac{1}{|t-s|^\alpha} dsdt \\
&= \frac{\tau^{1-\alpha}}{\Gamma(3-\alpha)} \left((k+1)^{2-\alpha} - 2k^{2-\alpha} + (k-1)^{2-\alpha}\right), \quad k \ge 1, \\
\tilde{b}_0 &= \frac{2}{\Gamma(2-\alpha)}\frac{1}{\tau} \int_0^\tau t^{1-\alpha} dt = \frac{2}{\Gamma(3-\alpha)} \tau^{1-\alpha}.
\end{aligned}$$

It is easy to see that $b_{|k|}$ is an approximation of $\tilde{b}_{|k|}$ by evaluating the integration using a one-sided quadrature rule. To prove that B is positive definite, we need to prove that the difference between B and $2A_\alpha/\tau$ in the off-diagonal parts can be controlled by the difference in the diagonal part. To show this, for the diagonal term we have

$$2b_0 - \tilde{b}_0 = \frac{2\tau^{1-\alpha}}{\Gamma(2-\alpha)} - \frac{2\tau^{1-\alpha}}{\Gamma(3-\alpha)} = 2b_0 \left(1 - \frac{1}{2-\alpha}\right) = \frac{2}{2-\alpha}\frac{\tau^{1-\alpha}}{\Gamma(1-\alpha)} \ge 0.$$

For the off-diagonal term, let $G(x) := \frac{1}{2-\alpha}(x+1)^{2-\alpha} - \frac{1}{2-\alpha}x^{2-\alpha}$; then we have

$$\begin{aligned}
&\tilde{b}_{|k|} - b_{|k|} \\
&= \frac{\tau^{1-\alpha}}{\Gamma(2-\alpha)} \left(\frac{(k+1)^{2-\alpha} - 2k^{2-\alpha} + (k-1)^{2-\alpha}}{2-\alpha} - \left[(k+1)^{1-\alpha} - k^{1-\alpha}\right] \right) \\
&= \frac{\tau^{1-\alpha}}{\Gamma(2-\alpha)} \left(G(k) - G(k-1) - G'(k)\right) \\
&= \frac{\tau^{1-\alpha}}{\Gamma(2-\alpha)} \frac{1}{2}(1-\alpha)\left(x^{-\alpha} - (x+1)^{-\alpha}\right) \quad \text{for some } x \in [k-1, k] \\
&\ge 0 \quad \forall\ k \ge 1.
\end{aligned}$$

Thus we obtain

$$\begin{aligned}
\sum_{k=1}^{m} \left|\tilde{b}_{|k|} - b_{|k|}\right| &= \frac{\tau^{1-\alpha}}{\Gamma(2-\alpha)} \left(\frac{(m+1)^{2-\alpha} - m^{2-\alpha} - 1}{2-\alpha} - \left[(m+1)^{1-\alpha} - 1\right] \right) \\
&\le \frac{\tau^{1-\alpha}}{\Gamma(1-\alpha)} \left(\frac{1}{2-\alpha} - \frac{1}{2}(m+1)^{-\alpha} \right), \quad 1 \le m \le n-1.
\end{aligned}$$

A direct calculation shows that the column sum of the off-diagonals is bounded by

$$c_0 := \frac{\tau^{1-\alpha}}{\Gamma(1-\alpha)}\left(\frac{2}{2-\alpha} - \left(\frac{n+1}{2}\right)^{-\alpha}\right).$$

Hence $C = \{c_{k-j}\}_{k,j=1}^{n}$ with $c_k = b_{|k|} - \tilde{b}_{|k|}$ for $k = \pm 1, \ldots, \pm n$ is a symmetric positive definite M-matrix. We then have

$$\begin{aligned} B &= \frac{2}{\tau}A_\alpha(u^n, u^n) + \sum_{k=1}^{n}\left[2b_0 - \tilde{b}_0 - c_0\right]u_k^2 + \sum_{k=1}^{n}\sum_{j=1}^{n} c_{k-j}u_k u_j \\ &\geq \frac{2}{\tau}A_\alpha(u^n, u^n) + \sum_{k=1}^{n}\left[2b_0 - \tilde{b}_0 - c_0\right]u_k^2 \\ &= \frac{2}{\tau}A_\alpha(u^n, u^n) + s_n\sum_{k=1}^{n} u_k^2. \end{aligned}$$

The proof is complete. ∎

We are now ready to give the following result indicating that the proposed numerical scheme is energy stable.

THEOREM 3.1. *The numerical solution of* (3.7) *with a modified bulk potential function* (3.6) *satisfies the following discrete energy dissipation law:*

$$\begin{aligned} E[\phi^n] - E[\phi^0] \leq & -\frac{b_0}{2\gamma\tau}\sum_{k=0}^{n-1}\|\delta_t\phi^{k+1}\|^2 \\ & -\sum_{k=0}^{n-1}\left\{\frac{\varepsilon}{2}\|\nabla\delta_t\phi^{k+1}\|^2 + \left\langle\frac{S}{\gamma} - \frac{1}{2\varepsilon}f'(\xi^k), (\delta_t\phi^{k+1})^2\right\rangle\right\}, \end{aligned} \tag{3.11}$$

where $\delta_t\phi^{k+1} := \phi^{k+1} - \phi^k$, *provided that*

$$S + \frac{b_0}{2\tau} \geq \frac{\gamma L}{2\varepsilon}, \tag{3.12}$$

where L *is given by* (3.5). *If* $S \geq \gamma L/2\varepsilon$, *then the scheme is unconditional energy stable in the sense that*

$$E[\phi^n] \leq E[\phi^0] \quad \forall\, \tau > 0,\, n > 0.$$

Proof. Multiplying both sides of (3.7) by $\delta_t\phi^{k+1}$ and integrating in space, we see that the resulting right-hand side is given by

$$\begin{aligned} \text{RHS} &= -\frac{\varepsilon}{2}\|\nabla\phi^{k+1}\|^2 + \frac{\varepsilon}{2}\|\nabla\phi^k\|^2 - \frac{\varepsilon}{2}\|\nabla\delta_t\phi^{k+1}\|^2 - \left\langle\frac{1}{\varepsilon}f(\phi^k)\delta_t\phi^{k+1} + \frac{S}{\gamma}(\delta_t\phi^{k+1})^2, 1\right\rangle \\ &= -\frac{\varepsilon}{2}\|\nabla\phi^{k+1}\|^2 + \frac{\varepsilon}{2}\|\nabla\phi^k\|^2 - \frac{\varepsilon}{2}\|\nabla\delta_t\phi^{k+1}\|^2 \\ &\quad - \left\langle\frac{1}{\varepsilon}F(\phi^{k+1}) - \frac{1}{\varepsilon}F(\phi^k) + \left(\frac{S}{\gamma} - \frac{1}{2\varepsilon}f'(\xi^k)\right)(\delta_t\phi^{k+1})^2, 1\right\rangle, \end{aligned}$$

where $\xi^k(x)$ is between $\phi^k(x)$ and $\phi^{k+1}(x)$. On the other hand, the resulting left-hand side is given by

$$\text{LHS} = \frac{1}{\gamma\tau}\int_\Omega \sum_{j=0}^{k} b_j\delta_t\phi^{k+1-j}\delta_t\phi^{k+1}dx.$$

Summing up both sides for $k = 0, \ldots, n-1$, we get

$$E[\phi^n] - E[\phi^0] = -\frac{1}{\gamma\tau}\int_\Omega \sum_{k=0}^{n-1}\sum_{j=0}^{k} b_j \delta_t \phi^{k+1-j}\delta_t\phi^{k+1}dx \\ - \sum_{k=0}^{n-1}\left\{\frac{\varepsilon}{2}\|\nabla\delta_t\phi^{k+1}\|^2 + \left\langle \frac{S}{\gamma} - \frac{1}{2\varepsilon}f'(\xi^k), (\delta_t\phi^{k+1})^2\right\rangle\right\}.$$

The desired energy estimate (3.11) follows by using Lemma 3.1. ∎

3.2. The time-fractional Cahn–Hilliard equation. The scheme (3.7) can be easily extended to the time-fractional CH equation (2.17) with the double-well potential function of quadratic growth (3.6) as follows:

$$\frac{1}{\gamma}\sum_{j=0}^{k} b_j \frac{\phi^{k+1-j}(x) - \phi^{k-j}(x)}{\tau} = \Delta\mu^{k+1}, \tag{3.13}$$

$$\mu^{n+1} = -\varepsilon\Delta\phi^{k+1} + \frac{1}{\varepsilon}f(\phi^k) + \frac{S}{\gamma}(\phi^{k+1} - \phi^k). \tag{3.14}$$

Similarly to the time-fractional AC equation case, we can prove the following energy dissipation property.

THEOREM 3.2. *Consider the numerical scheme* (3.13)–(3.14) *with a modified bulk potential function* (3.6). *Then the numerical solution of* (3.13)–(3.14) *satisfies the following discrete energy dissipation property:*

$$E[\phi^n] - E[\phi^0] \le -\frac{b_0}{2\gamma\tau}\sum_{k=0}^{n-1}\|\delta_t\phi^{k+1}\|^2_{H^{-1}} \\ - \sum_{k=0}^{n-1}\left\{\frac{\varepsilon}{2}\|\nabla\delta_t\phi^{k+1}\|^2 + \left\langle \frac{S}{\gamma} - \frac{1}{2\varepsilon}f'(\xi^k), (\delta_t\phi^{k+1})^2\right\rangle\right\}, \tag{3.15}$$

provided that $\sqrt{\frac{b_0\varepsilon}{\gamma\tau}} + \frac{S}{\gamma} \ge \frac{L}{2\varepsilon}$. *If* $S \ge \frac{\gamma L}{2\varepsilon}$, *then the scheme is unconditional energy stable in the sense that*

$$E[\phi^n] \le E[\phi^0] \quad \forall\, \tau > 0,\ n > 0.$$

3.3. The time-fractional molecular beam epitaxy equation. The scheme (3.7) and the relevant analysis also apply to the time-fractional MBE model (2.23) without slope selection, in which we have

$$\mathbf{f}_m'(\mathbf{v}) := \frac{\partial \mathbf{f}_m(\mathbf{v})}{\partial \mathbf{v}} = \frac{2\mathbf{v}^2 - (|\mathbf{v}|^2+1)I}{(1+|\mathbf{v}|^2)^2}, \tag{3.16}$$

where I is an identity matrix. The corresponding numerical scheme is

$$\frac{1}{\gamma}\sum_{j=0}^{k} b_j \frac{\phi^{k+1-j}(x) - \phi^{k-j}(x)}{\tau} \\ = -\varepsilon\Delta^2\phi^{k+1} + \frac{1}{\varepsilon}\nabla\cdot\mathbf{f}_m(\nabla\phi^k) + \frac{S}{\gamma}(\Delta\phi^{k+1} - \Delta\phi^k), \quad k \ge 0. \tag{3.17}$$

Similarly, we can prove the following energy dissipation property.

THEOREM 3.3. *Consider the time-fractional MBE model* (2.23) *with periodic boundary condition or no-flux boundary condition* (2.25). *Then the numerical scheme* (3.17) *satisfies the following discrete energy law:*

$$E_m[\phi^n] - E_m[\phi^0] \le -\frac{b_0}{2\gamma\tau}\sum_{k=0}^{n-1}\|\delta_t\phi^{k+1}\|^2 - \sum_{k=0}^{n-1}\frac{\varepsilon}{2}\|\nabla^2\delta_t\phi^{k+1}\|^2 - \sum_{k=0}^{n-1}\Big\langle\frac{S}{\gamma} - \frac{1}{2\varepsilon}\mathbf{f}_m{}'(\xi^k), (\nabla\delta_t\phi^{k+1})^2\Big\rangle, \tag{3.18}$$

provided that $\sqrt{\frac{b_0\varepsilon}{\gamma\tau}} + \frac{S}{\gamma} \ge \frac{1}{2\varepsilon}\lambda_{max}\big(\mathbf{f}_m'(\xi^k)\big)$. *Here* $\lambda_{max}\big(\mathbf{f}_m'(\xi^k)\big)$ *means the largest eigenvalue of the matrix* $\mathbf{f}_m'(\xi^k)$. *In particular, if we choose* $S \ge \frac{\gamma}{16\varepsilon}$, *then the numerical scheme* (3.17) *for the time-fractional MBE model without slope selection is unconditionally energy stable for any time step size.*

Proof. We remark that the inequality (3.18) can be obtained by the standard energy method, which is similar to the methods employed in the previous subsections. To make the last term in (3.18) nonnegative, we need only

$$\frac{S}{\gamma} - \frac{1}{2\varepsilon}\lambda_{\max}\big(\mathbf{f}_m'(\xi^k)\big) \ge 0.$$

A direct calculation using (3.16) shows that $\lambda_{\max}\big(\mathbf{f}_m'(\xi^k)\big) \le 1/8$. Consequently, the above inequality holds provided that $S \ge \frac{\gamma}{16\varepsilon}$. ∎

Remark 3.2. One can also resort to the convex-splitting approach [16, 17] to design energy stable schemes. Take the classical double-well potential (1.2) as an example, and let

$$f_i(\phi) = \phi^3, \quad f_e(\phi) = \phi. \tag{3.19}$$

For the time-fractional CH equation, the corresponding convex-splitting scheme reads

$$\frac{1}{\gamma}\sum_{j=0}^{k} b_j\frac{\phi^{k+1-j}(x) - \phi^{k-j}(x)}{\tau} = \Delta\mu^{k+1}, \tag{3.20}$$

$$\mu^{n+1} = -\varepsilon\Delta\phi^{k+1} + \frac{1}{\varepsilon}f_i(\phi^{k+1}) - \frac{1}{\varepsilon}f_e(\phi^k). \tag{3.21}$$

For the time-fractional MBE model with slope selection, the corresponding scheme yields

$$\frac{1}{\gamma}\sum_{j=0}^{k} b_j\frac{\phi^{k+1-j}(x) - \phi^{k-j}(x)}{\tau} = -\varepsilon\Delta^2\phi^{k+1} + \frac{1}{\varepsilon}\nabla\cdot f_i(\nabla\phi^{k+1}) - \frac{1}{\varepsilon}\nabla\cdot f_e(\nabla\phi^k), \quad k \ge 0. \tag{3.22}$$

Here $f_i(\mathbf{v}) = |\mathbf{v}|^2\mathbf{v}$. These schemes can be proved to be unconditionally stable, but at each time step we need to solve a nonlinear system.

4. Maximum principle for the Allen–Cahn equation. Similarly to the classical Allen–Cahn equation (see, e.g., [40]), we can establish a discrete maximum principle for the time-fractional AC equation. Note that if the discrete maximum principle is valid, then the global Lipschitz condition on f can be removed as the numerical solutions are bounded by the initial data. In other words, the modified bulk potential function (3.6) may not be needed; instead, the standard double-well potential (1.2) can be used.

Next, we show that scheme (3.7) with the standard double-well potential (1.2) satisfies a discrete maximum principle provided that the time step size is sufficiently small.

THEOREM 4.1. *Suppose $\phi_0 \in C^0$ and $M_1 \le \phi_0(x) \le M_2$ for all $x \in \bar{\Omega}$. Let $\{\phi^k, k \ge 1\}$ be the solution of the semidiscretized scheme* (3.7) *with a standard double-well potential that satisfies property* (2.11)*. If*

$$\frac{b_0 - b_1}{\tau} + S \ge \gamma \frac{\max_{M_1 \le u \le M_2} |f'(u)|}{\varepsilon}, \tag{4.1}$$

then we have

$$M_1 \le \phi^k(x) \le M_2 \quad \forall\ k \ge 1,\ x \in \bar{\Omega}. \tag{4.2}$$

Proof. We rewrite the scheme (3.7) using (3.3) as

$$\begin{aligned} &\frac{b_0}{\gamma\tau}\phi^{k+1} + \frac{S}{\gamma}\phi^{k+1} - \varepsilon\Delta\phi^{k+1} \\ &\quad = \frac{1}{\gamma\tau}\left[\sum_{j=0}^{k-1}(b_j - b_{j+1})\phi^{k-j} + b_k\phi^0\right] + \frac{S}{\gamma}\phi^k - \frac{1}{\varepsilon}f(\phi^k), \quad k \ge 0. \end{aligned} \tag{4.3}$$

We first consider the case $k = 0$. By using the fact that $f(\phi^k) = f(\phi^k) - f(M_2) = f'(\xi)(\phi^k - M_2)$, we obtain

$$\begin{aligned} &\frac{b_0}{\gamma\tau}\phi^1 + \frac{S}{\gamma}\phi^1 - \varepsilon\Delta\phi^1 \\ &= \frac{b_0}{\gamma\tau}\phi^0 + \frac{S}{\gamma}\phi^0 + \frac{1}{\varepsilon}f'(\xi)(M_2 - \phi^0) \\ &= \frac{b_0}{\gamma\tau}M_2 + \frac{S}{\gamma}M_2 + \left(\frac{1}{\varepsilon}f'(\xi) - \frac{S}{\gamma} - \frac{b_0}{\gamma\tau}\right)(M_2 - \phi^0) \\ &\le \frac{b_0}{\gamma\tau}M_2 + \frac{S}{\gamma}M_2. \end{aligned}$$

The last inequality is a result of condition (4.1). Now, let x_0 be a maximum point of ϕ^1; if $\phi^1(x_0) > M_2$, we get

$$\frac{b_0}{\gamma\tau}\phi^1 + \frac{S}{\gamma}\phi^1 - \varepsilon\Delta\phi^1 > \frac{b_0}{\gamma\tau}M_2 + \frac{S}{\gamma}M_2 \quad \text{at } x = x_0,$$

which contradicts the above inequality. Thus, we have $\max_{x\in\bar{\Omega}} \phi^1(x) \le M_2$.

Next, suppose $\max_{x\in\bar{\Omega}} \phi^j(x) \le M_2$ holds for $j = 0, \ldots, k$. Then by using (3.4),

the fact $f(\phi^k) = f(\phi^k) - f(M_2) = f'(\xi)(\phi^k - M_2)$, and the condition (4.1), we get

$$\begin{aligned}
&\frac{b_0}{\gamma\tau}\phi^{k+1} + \frac{S}{\gamma}\phi^{k+1} - \varepsilon\Delta\phi^{k+1} \\
&\le \frac{b_1}{\gamma\tau}M_2 + \frac{b_0 - b_1}{\gamma\tau}\phi^k + \frac{S}{\gamma}\phi^k + \frac{1}{\varepsilon}f'(\xi)(M_2 - \phi^k) \\
&= \frac{b_0}{\gamma\tau}M_2 + \frac{S}{\gamma}M_2 + \left(\frac{1}{\varepsilon}f'(\xi) - \frac{S}{\gamma} - \frac{b_0 - b_1}{\gamma\tau}\right)(M_2 - \phi^k) \\
&\le \frac{b_0}{\gamma\tau}M_2 + \frac{S}{\gamma}M_2.
\end{aligned}$$

Again, let x_0 be a maximum point of ϕ^{k+1}; if $\phi^{k+1}(x_0) > M_2$, we obtain

$$\frac{b_0}{\gamma\tau}\phi^{k+1} + \frac{S}{\gamma}\phi^{k+1} - \varepsilon\Delta\phi^{k+1} > \frac{b_0}{\gamma\tau}M_2 + \frac{S}{\gamma}M_2 \quad \text{at } x = x_0,$$

which contradicts the above inequality. Thus, we have $\max_{x\in\bar{\Omega}} \phi^{k+1}(x) \le M_2$. By mathematical induction, we have $\max_{x\in\bar{\Omega}} \phi^j(x) \le M_2$ for any $j \ge 1$. The lower bound can be proved similarly. ∎

It is well known that the solution of linear time-fractional parabolic equations admits some kind of initial singularity (see, e.g., [4, 7, 22, 35, 44, 46]):

$$\phi(t) \in C([0,T]), \quad |\phi_t| \le C_\alpha t^{\alpha-1}. \tag{4.4}$$

The well-posedness and the limited regularity of the time-fractional AC equation (2.9)–(2.10) with F satisfying (3.5) was studied recently by Jin, Li, and Zhou [23] in the setting of the nonlinear subdiffusion equation. It is proved in [23] that if $\phi_0 \in H_0^1(\Omega) \cap H^2(\Omega)$, then (2.9)–(2.10) admits a unique solution ϕ satisfying

$$\phi \in C^\alpha([0,T]; L^2(\Omega)) \cap C([0,T]; H_0^1(\Omega) \cap H^2(\Omega)), \quad \partial_t^\alpha \phi \in C([0,T]; L^2(\Omega)), \tag{4.5}$$

$$\partial_t\phi(t) \in L^2(\Omega) \quad \text{and} \quad \|\partial_t\phi(t)\|_{L^2(\Omega)} \le ct^{\alpha-1} \quad \text{for } t \in (0,T]. \tag{4.6}$$

Correspondingly, the numerical solutions of scheme (3.7) with a modified bulk potential function (3.6) can be proved to satisfy the following convergence property using the standard technique in [23]:

$$\max_{1\le n\le N} \|\phi(n\tau) - \phi^n\|_{L^2(\Omega)} \le c\tau^\alpha. \tag{4.7}$$

Since the piecewise extension $\phi_\tau(x,t) := (n + 1 - t/\tau)\phi^n + (t/\tau - n)\phi^{n+1}$ ($n\tau \le t \le n\tau + \tau$) converges to the weak solution $\phi(x,t)$ in $C([0,T]; L^2(\Omega))$, using the facts that ϕ_τ is bounded uniformly (Theorem 4.1) for sufficiently small τ and that ϕ is a continuous function yields the following maximum principle result.

THEOREM 4.2. *Let $\phi(x,t)$ be a weak solution of (2.9)–(2.10) with a potential function $F(\phi)$ described by (2.11). Suppose that $\phi(x,0) = \phi_0 \in H_0^1(\Omega) \cap H^2(\Omega)$, $\Omega \subset \mathbb{R}^d, d = 2,3$, and $M_1 \le \phi_0(x) \le M_2$ for all $x \in \bar{\Omega}$; then*

$$M_1 \le \phi(x,t) \le M_2 \quad \forall \text{ a.e. } (x,t) \in \bar{\Omega} \times [0,T].$$

Remark 4.1. The above theorem provides a maximum principle for the weak solution. On the other hand, we can also obtain a maximum principle directly for the

strong solution. Suppose the initial value ϕ_0 and the spatial domain Ω are sufficiently smooth such that the solution ϕ of (2.9)–(2.10) with a potential function $F(\phi)$ described by (2.11) satisfies

$$\Delta\phi \in C^0((0,T]\times\Omega), \qquad \phi_t \in C^0((0,T]\times\Omega), \quad \phi \in C^0([0,T]\times\Omega). \tag{4.8}$$

If the initial data is bounded, i.e., $M_1 \le \phi_0 \le M_2$ for all $x \in \Omega$, then one can use a standard technique to prove that

$$M_1 \le \phi(x,t) \le M_2 \quad \forall x \in \Omega, \;\; t > 0.$$

We point out that the regularity assumptions (4.8) have been shown to be reasonable recently, e.g., as reported in [15].

5. Numerical experiments. In this section, numerical schemes proposed in the previous section will be employed to study the coarsening rates of the time-fractional phase-field models. We solve the phase-field equations in $\Omega = [0, L_x] \times [0, L_y]$ with periodic boundary conditions. A Fourier–Galerkin method is used for the spatial discretization. To enhance the computational efficiency, the fast sum-of-exponential algorithm developed in [21] is used to evaluate the historical part of the time-fractional derivatives.

5.1. Numerical results for the time-fractional Allen–Cahn equation. In this case, we take $L_x = L_y = 2$, $\varepsilon = 0.05$, and $\gamma = 0.05$. The stabilization constant S in scheme (3.7) is chosen as $S = 0.1$. We use 128×128 Fourier modes in the physical domain and set the time step size as $\tau = 0.1$. The initial state is chosen as

$$\phi_0(x) = \tanh\left(\frac{1}{\sqrt{2}\varepsilon}\Big(r - \frac{1}{4} - \frac{1+\cos(4\theta)}{16}\Big)\right), \quad r = \sqrt{x^2+y^2},\ \theta = \arctan\frac{y}{x}. \tag{5.1}$$

The phase-field function and the energy evolution with various fractional orders α are investigated. Figure 1 presents the phase-field function ϕ with $\alpha = 0.3, 0.5, 1$ at different time levels. It is clearly seen that it takes a longer time to reach the equilibrium if α becomes smaller. This observation can be further verified by looking at the energy dissipation curves displayed in Figure 2. It is seen from this figure that the energy dissipation for the time-fractional AC equation has a long tail effect.

5.2. Numerical results for the time-fractional Cahn–Hilliard equation. In this case, we take $L_x = L_y = 2$, $\varepsilon = 0.05$, and $\gamma = \varepsilon^2$. A uniformly random distribution field in $[-1, 1]$ is taken as the initial state, and the stabilization constant in scheme (3.13)–(3.14) is chosen as $S = 0.01$. We use 256×256 Fourier modes for spatial discretization. The time step size is taken as $\tau = 0.001$. As shown in section 3, the numerical scheme is unconditionally stable if a suitable stabilization constant is used.

We investigate again the time variation for the phase-field function and the energy evolution with different values of fractional parameters. Figure 3 presents the phase-field function ϕ with $\alpha = 0.3, 0.5, 1$ at different time levels. Again it is observed that as α decreases, the relaxation time reaching the equilibrium increases. This assertion can be further verified by checking the energy dissipation curves presented in Figure 4(a). The overall energy dissipation process can be split into three stages. In the first stage, the bulk force is the driving force, and consequently small scale phase separations form. In the second stage, small structures interact with one another, so that an energy dissipation power law can be observed. In particular, the power law

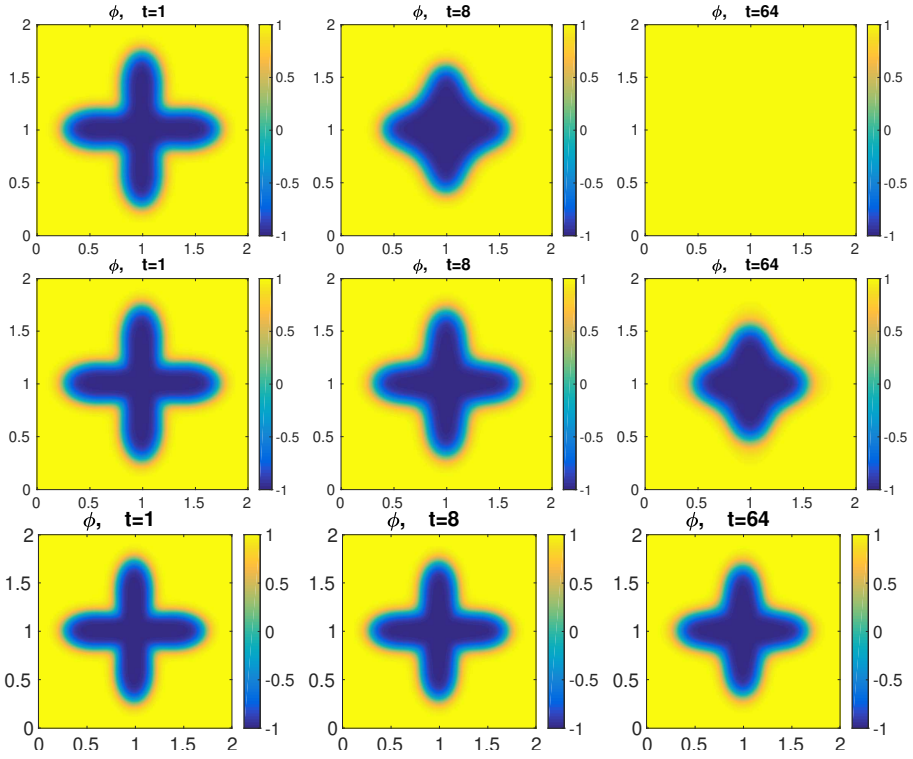

FIG. 1. *Snapshots of the solution of the time-fractional AC equation with* $\alpha = 1, 0.5, 0.3$ *(top, middle, and bottom rows, respectively).*

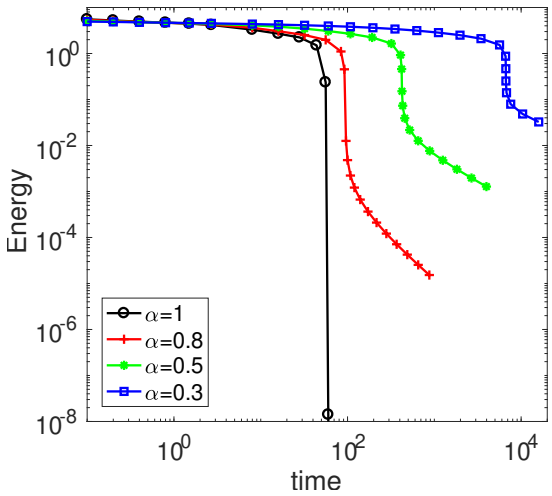

FIG. 2. *The energy dissipation for the time-fractional AC equation with different values of* α.

behaves like $E[\phi(t)] \approx C_\alpha t^{p_\alpha}$. It is found by data fitting that $p_\alpha \approx -\alpha/3$ (cf. Figure 4(b)), which is consistent with the $-1/3$ law for the classical CH equation (i.e., $\alpha = 1$). In the last stage, the equilibrium solution with the minimum energy is obtained.

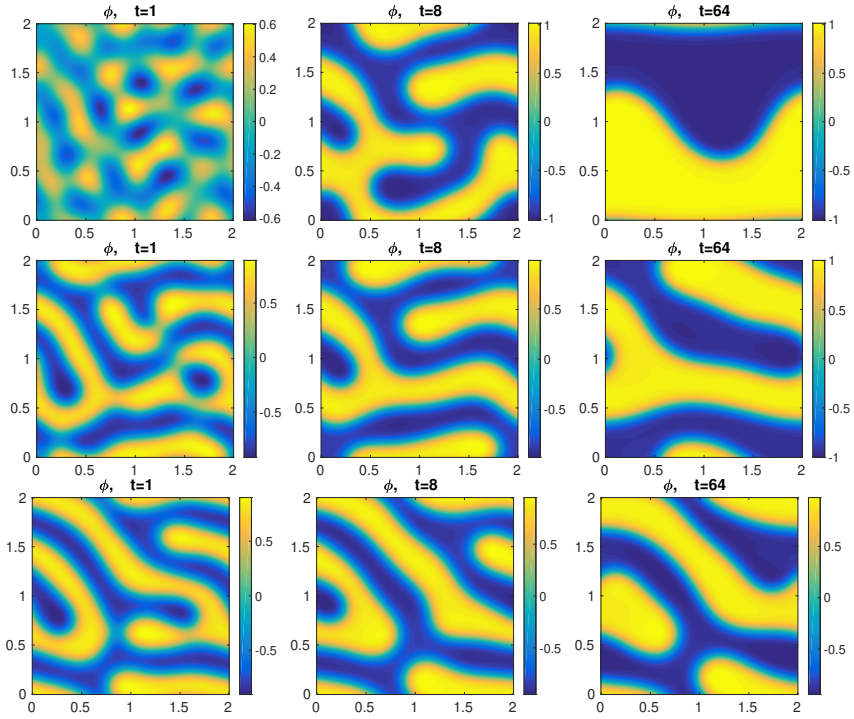

FIG. 3. *Snapshots of the solution of the time-fractional CH equation with* $\alpha = 1, 0.5, 0.3$ *(top, middle, and bottom rows, respectively).*

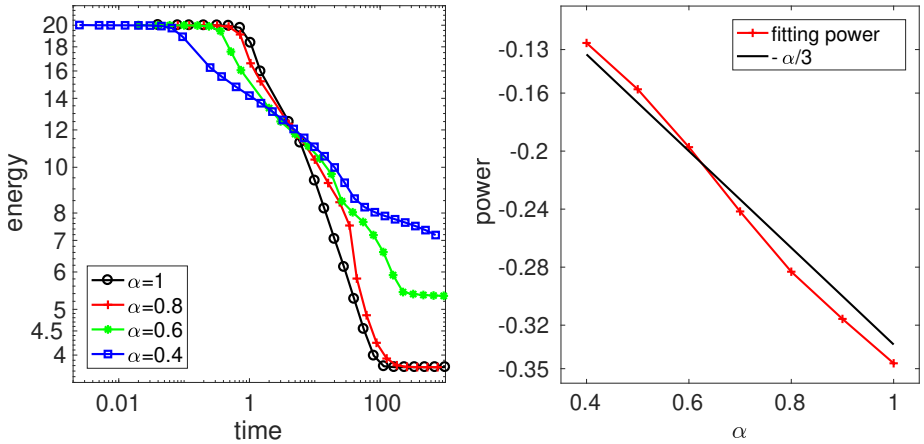

(a) The energy dissipation. (b) The power law.

FIG. 4. *The energy dissipation and the power law for the time-fractional CH equation with different values of* α.

5.3. Numerical results for the time-fractional molecular beam epitaxy model. For the time-fractional MBE model with slope selection, we take $L_x = L_y = 2\pi$, $\varepsilon = 0.1$, and $\gamma = \varepsilon$. A uniformly random distribution field in $[-0.001, 0.001]$ is chosen as the initial state. We use the stabilized scheme (3.17) with $S = 0.1$ and

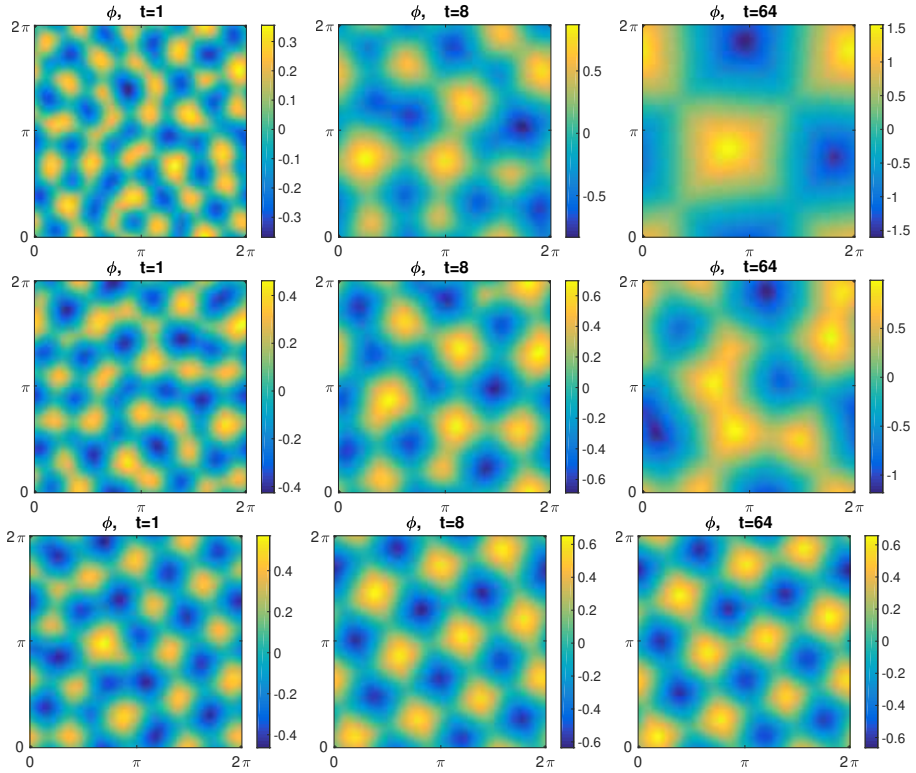

FIG. 5. *The snapshots of the numerical solution of the time-fractional MBE model with slope selection for* $\alpha = 1, 0.7,$ *and* 0.4 *(top, middle, and bottom rows, respectively).*

take 256×256 Fourier modes for spatial discretization. The time step size is taken as $\tau = 0.001$.

The time evolution for the phase-field function ϕ with $\alpha = 0.4, 0.7, 1$ is presented in Figure 5, which demonstrates again that as α decreases, the relaxation time reaching the equilibrium increases. It is seen from Figure 6(a) that the overall energy dissipation process for the time-fractional MBE model consists of three stages, and in the second stage a power law with an asymptotic power of $-\alpha/3$ is observed, which is confirmed numerically by Figure 6(b).

6. Concluding remarks. In this work, we established an energy dissipation theory for the time-fractional phase-field equations. We prove in the continuous level that the time-fractional phase-field equations admit an energy dissipation law of integral type. In the discrete level, we propose a class of finite difference schemes that can inherit the discrete energy dissipation property. These numerical schemes are applied and analyzed for the time-fractional AC equation, the time-fractional CH equation, and the time-fractional MBE model. Several numerical experiments are carried out to verify the theoretical predictions. In particular, it is observed numerically that the energy dissipation rate satisfies a power law with an asymptotic power $-\alpha/3$, where α is the fractional parameter.

We conclude this work by pointing out several relevant issues which require further study:

- As discussed in Remark 2.1, we have presented the energy law $E[\phi(T)] \leq$

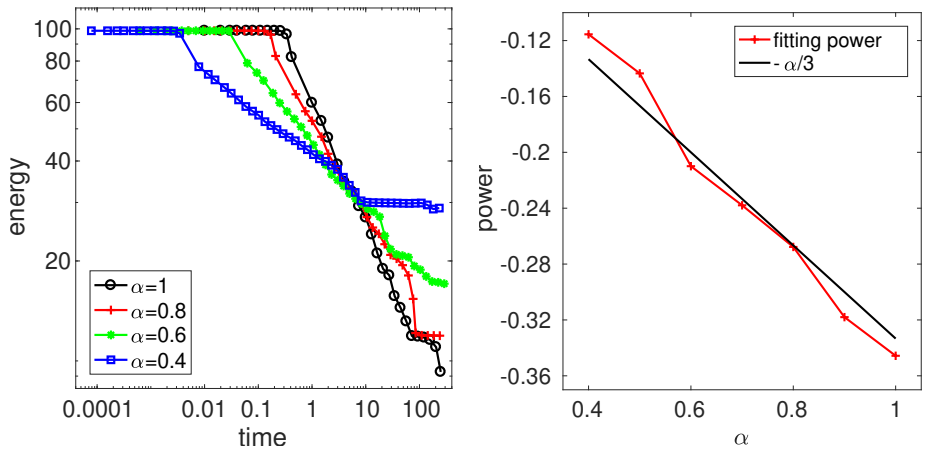

(a) The energy dissipation. (b) The power law scaling.

FIG. 6. *The energy dissipation and power-law scaling for time-fractional MBE model with slope selection at several values of* α.

$E[\phi(0)]$. An open question is to verify the following energy dissipation law:

$$\frac{d}{dt}E \le 0 \quad \text{or} \quad \frac{d^\alpha}{dt^\alpha}E \le 0.$$

- We have shown numerically that the energy dissipation rate satisfies a power law with an asymptotic power $-\alpha/3$ in the coarsening stage for the time-fractional CH equation and the MBE model. However, a rigorous theoretical justification is needed.
- On the numerical side, only first order schemes are investigated in this work. It will be more useful and more challenging to design high order energy stable schemes in our future studies.

Acknowledgments. We thank the anonymous referees for their valuable comments and suggestions which helped us to improve the manuscript. We also would like to thank Prof. Jie Shen, Prof. Yifa Tang, Dr. Jiwei Zhang, Dr. Zhi Zhou, and Dr. Honglin Liao for helpful discussions. The computations were partly done on the high performance computers of State Key Laboratory of Scientific and Engineering Computing, Chinese Academy of Sciences.

REFERENCES

[1] M. AINSWORTH AND Z. MAO, *Analysis and approximation of a fractional Cahn–Hilliard equation*, SIAM J. Numer. Anal., 55 (2017), pp. 1689–1718 https://doi.org/10.1137/16M1075302.

[2] M. AINSWORTH AND Z. MAO, *Well-posedness of the Cahn-Hilliard equation with fractional free energy and its Fourier Galerkin approximation*, Chaos Soliton. Fract., 102 (2017), pp. 264–273.

[3] G. AKAGI, G. SCHIMPERNA, AND A. SEGATTI, *Fractional Cahn-Hilliard, Allen-Cahn and porous medium equations*, J. Differential Equations, 261 (2016), pp. 2953–2985.

[4] M. ALLEN, L. CAFFARELLI, AND A. VASSEUR, *A parabolic problem with a fractional time derivative*, Arch. Rational Mech. Anal., 221 (2016), pp. 603–630, https://doi.org/10.1007/s00205-016-0969-z.

[5] S. ALLEN AND J. CAHN, *A microscopic theory for antiphase boundary motion and its application to antiphase domain coarsening*, Acta Metall., 27 (1979), pp. 1085–1095.

[6] J. Bosch, C. Kahle, and M. Stoll, *Preconditioning of a coupled Cahn-Hilliard Navier-Stokes system*, Commun. Comput. Phys., 23 (2018), pp. 603–628.

[7] H. Brunner, *Collocation Methods for Volterra Integral and Related Functional Differential Equations*, Cambridge Monogr. Appl. Comput. Math. 15, Cambridge University Press, 2004.

[8] L. A. Caffarelli and N. E. Muler, *An L^∞ bound for solutions of the Cahn-Hilliard equation*, Arch. Rational Mech. Anal., 133 (1995), pp. 129–144, https://doi.org/10.1007/BF00376814.

[9] J. W. Cahn and J. E. Hilliard, *Free energy of a nonuniform system* I*: Interfacial free energy*, J. Chem. Phys., 28 (1958), pp. 258–267.

[10] S. Clarke and D. D. Vvedensky, *Origin of reflection high-energy electron-diffraction intensity oscillations during molecular-beam epitaxy: A computational modeling approach*, Phys. Rev. Lett., 58 (1987), pp. 2235–2238.

[11] N. Condette, C. Melcher, and E. Süli, *Spectral approximation of pattern-forming nonlinear evolution equations with double-well potentials of quadratic growth*, Math. Comp., 80 (2011), pp. 205–223, https://doi.org/10.1090/S0025-5718-10-02365-3.

[12] A. E. Diegel, C. Wang, X. Wang, and S. M. Wise, *Convergence analysis and error estimates for a second order accurate finite element method for the Cahn-Hilliard-Navier-Stokes system*, Numer. Math., 137 (2017), pp. 495–534, https://doi.org/10.1007/s00211-017-0887-5.

[13] Q. Du, C. Liu, and X. Wang, *A phase field approach in the numerical study of the elastic bending energy for vesicle membranes*, J. Comput. Phys., 198 (2004), pp. 450–468, https://doi.org/10.1016/j.jcp.2004.01.029.

[14] Q. Du and R. A. Nicolaides, *Numerical analysis of a continuum model of phase transition*, SIAM J. Numer. Anal., 28 (1991), pp. 1310–1322, https://doi.org/10.1137/0728069.

[15] Q. Du, J. Yang, and Z. Zhou, *Time-Fractional Allen-Cahn Equations: Analysis and Numerical Methods*, preprint, https://arxiv.org/abs/1906.06584, 2019.

[16] C. M. Elliott and A. M. Stuart, *The global dynamics of discrete semilinear parabolic equations*, SIAM J. Numer. Anal., 30 (1993), pp. 1622–1663, https://doi.org/10.1137/0730084.

[17] D. J. Eyre, *Unconditionally gradient stable time marching the Cahn-Hilliard equation*, in Computational and Mathematical Models of Microstructural Evolution (San Francisco, CA, 1998), Mater. Res. Soc. Sympos. Proc. 529, MRS, 1998, pp. 39–46.

[18] H. Gomez and T. Hughes, *Provably unconditionally stable, second-order time-accurate, mixed variational methods for phase-field models*, J. Comput. Phys., 230 (2011), pp. 5310–5327.

[19] J. Guo, C. Wang, S. Wise, and X. Yue, *An H^2 convergence of a second-order convex-splitting, finite difference scheme for the three-dimensional Cahn–Hilliard equation*, Commun. Math. Sci., 14 (2016), pp. 489–515, https://doi.org/10.4310/CMS.2016.v14.n2.a8.

[20] A. Hawkins-Daarud, K. G. V. D. Zee, and J. T. Oden, *Numerical simulation of a thermodynamically consistent four-species tumor growth model*, Int. J. Numer. Methods Biomed. Eng., 8 (2012), pp. 3–24.

[21] S. Jiang, J. Zhang, Q. Zhang, and Z. Zhang, *Fast evaluation of the Caputo fractional derivative and its applications to fractional diffusion equations*, Commun. Comput. Phys., 21 (2017), pp. 650–678, https://doi.org/10.4208/cicp.OA-2016-0136.

[22] B. Jin, R. Lazarov, and Z. Zhou, *Error estimates for a semidiscrete finite element method for fractional order parabolic equations*, SIAM J. Numer. Anal., 51 (2013), pp. 445–466, https://doi.org/10.1137/120873984.

[23] B. Jin, B. Li, and Z. Zhou, *Numerical analysis of nonlinear subdiffusion equations*, SIAM J. Numer. Anal., 56 (2018), pp. 1–23, https://doi.org/10.1137/16M1089320.

[24] A. Kilbas, H. Srivastava, and J. Trujillo, *Theory and Applications of Fractional Differential Equations*, North-Holland Math. Stud. 204, Elsevier Science B.V., 2006.

[25] K. N. Le, W. McLean, and K. Mustapha, *Numerical solution of the time-fractional Fokker–Planck equation with general forcing*, SIAM J. Numer. Anal., 54 (2016), pp. 1763–1784, https://doi.org/10.1137/15M1031734.

[26] B. Li and J.-G. Liu, *Thin film epitaxy with or without slope selection*, Eur. J. Appl. Math., 14 (2003), pp. 713–743.

[27] X. Li, V. Cristini, Q. Nie, and J. Lowengrub, *Nonlinear three-dimensional simulation of solid tumor growth*, Discrete Contin. Dyn. Syst. Ser. B, 7 (2007), pp. 581–604.

[28] Z. Li, H. Wang, and D. Yang, *A space-time fractional phase-field model with tunable sharpness and decay behavior and its efficient numerical simulation*, J. Comput. Phys., 347 (2017), pp. 20–38.

[29] H. Liao, W. McLean, and J. Zhang, *A discrete Grönwall inequality with applications to numerical schemes for subdiffusion problems*, SIAM J. Numer. Anal., 57 (2019), pp. 218–237, https://doi.org/10.1137/16M1175742.

[30] Y. Lin and C. Xu, *Finite difference/spectral approximations for the time-fractional diffusion equation*, J. Comput. Phys., 225 (2007), pp. 1533–1552, https://doi.org/10.1016/j.jcp.2007.02.001.

[31] J. Lowengrub and L. Truskinovsky, *Quasi-incompressible Cahn-Hilliard fluids and topological transitions*, R. Soc. Lond. Proc. Ser. A Math. Phys. Eng. Sci, 454 (1998), pp. 2617–2654.

[32] L. Ma, R. Chen, X. Yang, and H. Zhang, *Numerical approximations for Allen-Cahn type phase field model of two-phase incompressible fluids with moving contact lines*, Commun. Comput. Phys., 27 (2017), pp. 867–889.

[33] D. M. Anderson, G. B. McFadden and A. A. Wheeler, *Diffuse-interface methods in fluid mechanics*, Annu. Rev. Fluid Mech., 30 (1998), pp. 139–165.

[34] W. McLean and K. Mustapha, *Convergence analysis of a discontinuous Galerkin method for a sub-diffusion equation*, Numer. Algorithms, 52 (2009), pp. 69–88, https://doi.org/10.1007/s11075-008-9258-8.

[35] K. Mustapha and D. Schötzau, *Well-posedness of hp-version discontinuous Galerkin methods for fractional diffusion wave equations*, IMA J. Numer. Anal., 34 (2014), pp. 1426–1446, https://doi.org/10.1093/imanum/drt048.

[36] Y. Nec, A. Nepomnyashchy, and A. Golovin, *Front-type solutions of fractional Allen-Cahn equation*, Phys. D, 237 (2008), pp. 3237–3251.

[37] J. A. Nohel and D. F. Shea, *Frequency domain methods for Volterra equations*, Adv. Math., 22 (1976), pp. 278–304, https://doi.org/10.1016/0001-8708(76)90096-7.

[38] I. Podlubny, *Fractional Differential Equations*, Elsevier, 1998.

[39] T. Qian, X.-P. Wang, and P. Sheng, *Molecular scale contact line hydrodynamics of immiscible flows*, Phys. Rev. E, 68 (2003), 016306, http://pre.aps.org/abstract/PRE/v68/i1/e016306.

[40] J. Shen, T. Tang, and J. Yang, *On the maximum principle preserving schemes for the generalized Allen-Cahn equation*, Commun. Math. Sci., 14 (2016), pp. 1517–1534, https://doi.org/10.4310/CMS.2016.v14.n6.a3.

[41] J. Shen and X. Yang, *Numerical approximations of Allen-Cahn and Cahn-Hilliard equations*, Discrete Contin. Dyn. Syst., 28 (2010), pp. 1669–1691.

[42] J. Shen, X. Yang, and H. Yu, *Efficient energy stable numerical schemes for a phase field moving contact line model*, J. Comput. Phys., 284 (2015), pp. 617–630, https://doi.org/10.1016/j.jcp.2014.12.046.

[43] F. Song, C. Xu, and G. E. Karniadakis, *A fractional phase-field model for two-phase flows with tunable sharpness: Algorithms and simulations*, Comput. Methods Appl. Mech. Engrg., 305 (2016), pp. 376–404.

[44] M. Stynes, E. O'Riordan, and J. L. Gracia, *Error analysis of a finite difference method on graded meshes for a time-fractional diffusion equation*, SIAM J. Numer. Anal., 55 (2017), pp. 1057–1079, https://doi.org/10.1137/16M1082329.

[45] Z.-Z. Sun and X. Wu, *A fully discrete difference scheme for a diffusion-wave system*, Appl. Numer. Math., 56 (2006), pp. 193–209, https://doi.org/10.1016/j.apnum.2005.03.003.

[46] T. Tang, *A finite difference scheme for partial integro-differential equations with a weakly singular kernel*, Appl. Numer. Math., 11 (1993), pp. 309–319, https://doi.org/10.1016/0168-9274(93)90012-G.

[47] L. Wang and H. Yu, *Energy stable second order linear schemes for the Allen-Cahn phase-field equation*, Commun. Math. Sci., 17 (2018), pp. 609–635, https://doi.org/10.4310/CMS.2019.v17.n3.a2.

[48] L. Wang and H. Yu, *On efficient second order stabilized semi-implicit schemes for the Cahn–Hilliard phase field equation*, J. Sci. Comput., 77 (2018), pp. 1185–1209, https://doi.org/10.1007/s10915-018-0746-2.

[49] S. M. Wise, J. S. Lowengrub, H. B. Frieboes, and V. Cristini, *Three-dimensional multispecies nonlinear tumor growth* I*: Model and numerical method*, J. Theor. Biol., 253 (2008), pp. 524–543, https://doi.org/10.1016/j.jtbi.2008.03.027.

[50] C. Xu and T. Tang, *Stability analysis of large time-stepping methods for epitaxial growth models*, SIAM J. Numer. Anal., 44 (2006), pp. 1759–1779, https://doi.org/10.1137/050628143.

[51] X. Xu, Y. Di, and H. Yu, *Sharp-interface limits of a phase-field model with a generalized Navier slip boundary condition for moving contact lines*, J. Fluid Mech., 849 (2018), pp. 805–833, https://doi.org/10.1017/jfm.2018.428.

[52] Y. Yan, W. Chen, C. Wang, and S. M. Wise, *A second-order energy stable BDF numerical scheme for the Cahn-Hilliard equation*, Commun. Comput. Phys., 23 (2018), pp. 572–602.

[53] H. Yu, G. Ji, and P. Zhang, *A nonhomogeneous kinetic model of liquid crystal polymers and its thermodynamic closure approximation*, Commun. Comput. Phys., 7 (2010), pp. 383–402.

[54] J. Zhao, L. Chen, and H. Wang, *On power law scaling dynamics for time-fractional phase field models during coarsening*, Commun. Nonlinear Sci., 70 (2019), pp. 257–270.